
Journal Offprint Paper

BUTTERWORTH
HEINEMANN

 A member of the Reed Elsevier group

Linacre House, Jordan Hill, Oxford OX2 8DP, UK

OFFPRINT PAPERS

Butterworth-Heinemann are leading international publishers of a range of highly respected academic journals in Applied Science, Information Technology, Engineering, Materials Science, Policy Studies, Social Sciences, Biomedical Sciences and Medicine. Our journals are renowned for their high quality of both content and presentation. Papers are peer-reviewed and all our journals have distinguished editorial boards.

If you would like to receive subscription details, a sample copy or other information about the journal in which this offprint appeared, please complete and return the form provided below. Information about our other titles is available from our price list or catalogue (see form below).

Notes for Authors

To obtain details on how to submit papers to one of our journals, please contact:

The Group Editor at the Oxford address below (please state the appropriate journal title).

Reprints

We can reprint any article appearing in our journals and tailor it to your needs with an advert or logo. For a quotation on your reprint requirements, please contact: **The Reprints Department** at the Oxford address below.

For further information about any other aspect of our journals, please contact us at:
Butterworth-Heinemann Ltd., Linacre House, Jordan Hill, Oxford, OX2 8DP, UK
Tel: +44 (0) 865 310366 Fax: +44 (0) 865 310898

✂ Please cut here

Return Form

Area(s) of Interest:

Journal Title(s)
.....

Subscription Details Request

Please send me full subscription details and information about the above journal title(s)

Sample Copy Request Form

Please send me a free sample copy of the above journal title(s)

Journals Price List

Please send me a full price list for all your journals

Catalogue

Please send me a catalogue of your journals

Name

Organisation

Address

Postcode / Zipcode Country

Telephone E-mail

Fax Signature Date

Please return this form to:

Butterworth-Heinemann Ltd.
Turpin Distribution Services Ltd.
Blackhorse Road
Letchworth
Herts, SG6 1HN, UK
Tel: +44 (0) 462 672555
Fax: +44 (0) 462 480947

OR

Journal Fulfilment Department
Butterworth-Heinemann US
80 Montvale Avenue
Stoneham
MA 02180, USA
Tel: +1 617 438 8464
Fax: +1 617 438 1479



A word from the Director

With the end of the summer in the northern hemisphere, a new academic year has begun. In companies, too, sunny holidays are over for many people. Autumn is always an occasion for a good start. I hope that UV radiation and global warming did not spoil anyone's vacation!

News from Eastern Africa, Southern Europe and, unfortunately, from many other places in the world have reminded us of the challenges and risks of our time, as well as of the necessity of assuring economic growth, which is the first requirement for peace, and for which we all have to work hard.

Of course, it occurs to us that one way to do this is to develop the means for producing refrigeration in the food sector and in air conditioning. After the Hannover meeting*, which was the subject of the last 'A word from the Director', many IIR members met again in the United States, at Purdue University, south of Chicago, where these topics were dealt with, along with the problems of noise in compressors. The next important date is set for Padua, Italy, in September 1994, for the meeting on 'CFCs: the day after'. You will hear more about this in a future issue of the IJR.

However, the use of refrigeration is not being neglected, for all that. During the meeting in Istanbul, Turkey, last June, advances in cold treatment and preservation of food products were discussed, along with the problems of predicting microbiological changes. Meetings in Brest, France, and Mendoza, Argentina, will focus on vegetables and stone fruits.

Helium, which plays a major role in cryogenics, was the subject of 'Helium 94', in Moscow, Russia, where Professor Arkharov, President of Section A, represented the IIR; this has both technical and geopolitical implications.

All these areas will be discussed at the XIXth International Congress of Refrigeration in The Hague in 1995, and I invite you to attend and review, once again, the latest developments.

*Most preprints now available at the IIR.

Le mot du Directeur L. Lucas

Avec la fin de l'été dans l'hémisphère nord, une nouvelle année universitaire et scolaire a commencé. Dans les entreprises aussi, beaucoup ont eu quelques vacances ensoleillées. C'est toujours une occasion pour faire le point pour un nouveau départ. J'espère que les U.V. et le réchauffement planétaire ne les ont pas trop perturbés!

Les nouvelles d'Afrique de l'Est, d'Europe du Sud et, hélas, de bien d'autres endroits, étaient là pour nous rappeler les enjeux et les risques de notre époque ainsi que les exigences du développement économique, première condition de la paix, auquel nous pouvons tous contribuer.

La mise au point de nouveaux procédés de production du froid dans l'alimentaire et en conditionnement d'air en est bien sûr l'un des moyens. Après la réunion d'Hanovre (1), dont le dernier 'mot du Directeur' nous rendait compte, beaucoup de membres de l'IIF se sont retrouvés aux Etas-Unis pour en parler, à l'Université de Purdue, au Sud de Chicago, où ces thèmes alternaient notamment avec les problèmes du bruit dans les compresseurs. Le prochain grand rendez-vous est celui de Padoue en Italie: 'l'après CFC', en septembre. Un prochain numéro vous en parlera.

L'utilisation du froid n'en est pas négligée pour autant. La réunion d'Istanbul en Turquie en juin a permis de se pencher sur les nouveautés relatives au traitement et à la conservation des produits alimentaires par le froid. Ont été abordés les problèmes de prédiction du développement microbologique. Les réunions de Brest et de Mendoza (Argentine) se focalisent sur les légumes et sur les fruits à noyaux.

Le problème du l'hélium, majeur pour la cryogénie, traité à 'Helium 94', à Moscou, où le Professeur Arkharov, président de la Section A, représentait l'IIF, nous ramenait à des questions à la fois techniques et géopolitiques.

L'ensemble de ces problèmes se retrouveront au XIXe Congrès International du Froid de la Haye, où je vous invite à faire à nouveau le point l'été prochain.

(1) des exemplaires de la plupart des preprints sont déjà disponibles à l'IIF.

Dedicated mechanical subcooling design strategies for supermarket applications

J. W. Thornton, S. A. Klein and J. W. Mitchell

Solar Energy Laboratory, University of Wisconsin-Madison, Madison, WI 53706, USA

Received 4 January 1993; revised 29 April 1994

Dedicated mechanical subcooling cycles utilize a small mechanical vapour-compression cycle, coupled to the main cycle at the exit of the condenser, to provide subcooling to the main refrigeration cycle. The amount of subcooling, the thermal lift of the subcooling cycle, and consequently the performance of the overall cycle, can be directly related to the temperature of the subcooling cycle evaporator. In this paper, the optimum value of the subcooling evaporator temperature is predicted using an ideal dedicated subcooling cycle. These results are then compared with those generated from a property-dependent model. The consideration of this optimum subcooling evaporator temperature leads to a design rule for the optimum distribution of heat exchange area for the dedicated subcooling cycle.

(Keywords: refrigeration cycle; compression; subcooling; mechanical subcooling; optimization; supermarket)

Stratégies de conception de systèmes spécialisés de sous-refroidissement mécanique pour les supermarchés

Les cycles spécialisés de sous-refroidissement mécanique utilisent un petit cycle mécanique de compression de vapeur relié au cycle principal à la sortie du compresseur, pour sous-refroidir le cycle frigorifique principal. La quantité de chaleur du sous-refroidissement, son écart de température, et par conséquent la performance de l'ensemble du cycle peuvent dépendre directement de la température de l'évaporateur de cycle de sous-refroidissement. Dans cet article, on prévoit la valeur optimale de la température de l'évaporateur de sous-refroidissement en utilisant un cycle idéal de sous-refroidissement. On compare ensuite ces résultats à ceux obtenus par un modèle de simulation d'un système concret (supermarché). La considération de cette température optimale de l'évaporateur de sous-refroidissement conduit à adopter une règle de conception pour la répartition optimale des échanges thermiques dans le cycle de sous-refroidissement.

(Mots clés: cycle frigorifique; compression; sous-refroidissement; sous-refroidissement mécanique; optimisation; supermarché)

The coefficient of performance (COP) and capacity of low-temperature refrigeration cycles can be increased beyond that which is possible through standard vapour-compression cycles by utilizing dedicated mechanical subcooling. Dedicated mechanical subcooling cycles employ a second vapour-compression cycle solely for the purpose of providing subcooling to the main refrigeration cycle. The subcooling cycle is coupled to the main cycle by the use of a subcooler located at the discharge of the main cycle condenser (*Figure 1*). For supermarket applications, the subcooler, which acts as the evaporator for the subcooling cycle, provides about 40 °C of subcooling to the main cycle at design conditions. Because the subcooling cycle provides a lower-temperature sink, the main cycle is able to realize a gain in capacity and COP, particularly at high ambient and low evaporator temperatures. In practice, the components of the subcooling cycle are a fraction of the size of the main cycle components and perform through much smaller temperature extremes. For this reason, the COP of the subcooling cycle is appreciably higher than that of the main refrigeration cycle, resulting in an increase in the

overall cycle COP. Using a computer model, Couvillion *et al.*¹ predicted improvements in COP ranging from 6 to 82%, and in capacity from 20 to 170%. The present study extends previous investigations by determining optimum subcooling temperatures and heat exchanger designs necessary to achieve this performance improvement.

A pressure-enthalpy diagram for a dedicated mechanical subcooling cycle is shown in *Figure 2*. Subcooling allows the refrigerant to enter the main cycle evaporator with a lower quality (point 4) compared with a typical vapour-compression cycle (point 4'). The lower quality of the evaporator inlet corresponds to an increase in the refrigeration capacity per unit mass of refrigerant circulated. However, the increase in refrigeration capacity is not without cost. Neglecting losses to the environment, an energy balance on the subcooler indicates that the amount of subcooling provided to the main cycle must equal the heat addition to the subcooling cycle evaporator. The heat addition to the subcooling cycle evaporator must be rejected in the subcooling cycle condenser at the cost of the work of the subcooling cycle compressor. Therefore there is a trade-off between the amount of

Nomenclature

C_{min}	Mass flowrate-specific heat product of main cycle refrigerant	$\dot{Q}_{evap,main,no\ sub}$	Heat transfer rate to the main cycle evaporator if there is no subcooling
COP	Coefficient of performance	$\dot{Q}_{evap,sub}$	Heat transfer rate to the subcooling cycle evaporator
COP_{Carnot}	Ideal coefficient of performance	\dot{Q}_{sub}	Heat transfer rate across the subcooler
COP_{main}	Coefficient of performance of the main refrigeration cycle	s_i	Specific entropy at state point i in Figure 1
COP_{sub}	Coefficient of performance of the subcooling refrigeration cycle	T_L	Temperature of the refrigerated space
COP_{total}	Coefficient of performance of the overall dedicated subcooling cycle	T_H	Refrigeration cycle sink temperature
h_i	Specific enthalpy at state point i in Figure 1	T_M	Intermediate temperature for the ideal subcooling cycle
LMTD	Log mean temperature difference	UA	Overall heat transfer coefficient
\dot{m}_{ratio}	Refrigerant flow rate ratio	\dot{W}_{main}	Power required to operate main refrigeration cycle
$\dot{m}_{ref,main}$	Refrigerant flow rate for the main refrigeration cycle	\dot{W}_{sub}	Power required to operate subcooling refrigeration cycle
$\dot{m}_{ref,sub}$	Refrigerant flow rate for the subcooling refrigeration cycle	ϵ	Subcooler heat exchanger effectiveness
\dot{Q}_{evap}	Heat transfer rate to the main cycle evaporator	η	Isentropic efficiency

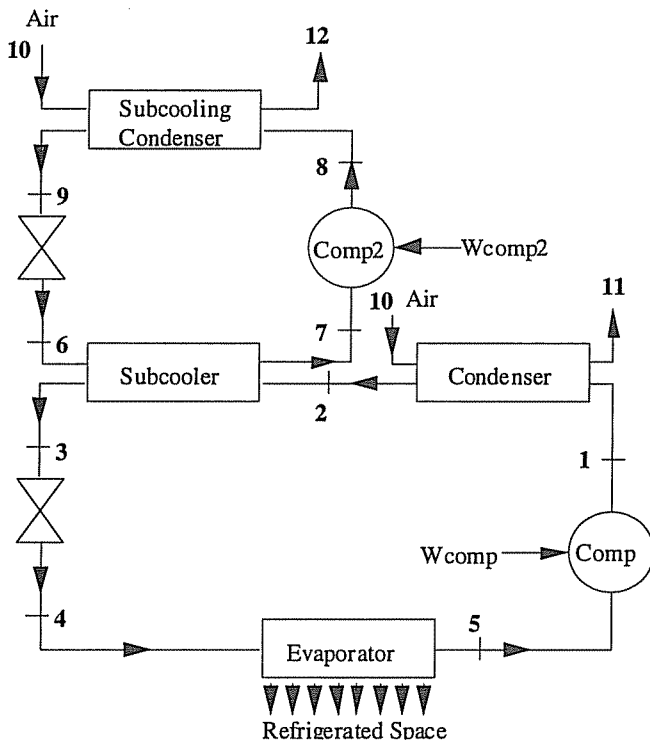


Figure 1 Component diagram for dedicated mechanical subcooling cycle

Figure 1 Diagramme des composants pour le cycle auxiliaire de sous-refroidissement mécanique

subcooling provided to the main cycle and the amount of work performed by the subcooling cycle compressor. This paper investigates this trade-off and explores the concept of the 'optimum' temperature for the subcooling cycle evaporator which is the temperature at which the COP of the overall cycle is maximized. The 'optimum' temperature is derived for a thermodynamically ideal mechanical subcooling refrigeration cycle. The results are then compared with those from a more detailed

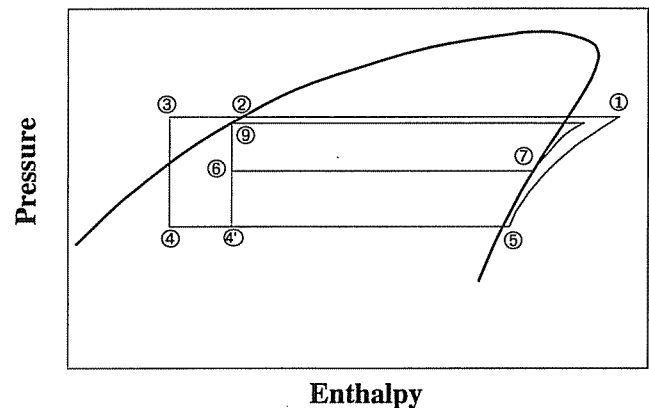


Figure 2 Pressure-enthalpy diagram for a dedicated mechanical subcooling cycle

Figure 2 Diagramme de pression-enthalpie pour un cycle auxiliaire de sous-refroidissement mécanique

property-dependent system model. Finally, design guidelines for the optimum distribution of heat exchange area for the dedicated mechanical subcooling cycle are developed.

Optimum temperature for a thermodynamically ideal cycle

The thermodynamically ideal mechanical subcooling cycle was developed using a Carnot cycle and classic heat exchanger theory. The Carnot cycle provides a theoretical upper limit on the performance of a refrigeration cycle with a COP given by

$$COP_{Carnot} = \frac{Capacity}{Power} = \frac{\dot{Q}_{evap}}{W} = \frac{T_L}{T_H - T_L} \quad (1)$$

The following assumptions were made in the development of the ideal mechanical subcooling model:

1. Both the main and subcooling cycle condensers reject heat at the sink temperature T_H .

2. The main cycle heat addition occurs at T_L , the refrigerated space temperature.
3. The subcooling cycle heat addition occurs at T_M , an intermediate temperature ($T_L \leq T_M \leq T_H$).
4. The COP of the main cycle and subcooling cycle are assumed to be the Carnot COP if no subcooling is provided.
5. There is no thermal energy loss to the environment in the subcooler.
6. The only irreversibility is due to the subcooler heat transfer.
7. The main cycle compressor work is not influenced by the amount of subcooling provided to the main cycle.
8. The exit states of the main cycle condenser and evaporator are unaffected by the amount of subcooling performed.
9. Isentropic expansion and compression are assumed for both the main and subcooling cycles.

If no subcooling is provided to the main cycle, the COP can be written as

$$\text{COP}_{\text{main}} = \frac{\dot{Q}_{\text{evap,main,no sub}}}{\dot{W}_{\text{main}}} = \frac{T_L}{T_H - T_L} \quad (2)$$

When subcooling is added to the main cycle, the refrigeration capacity will increase due to the reduced quality of the refrigerant entering the main cycle evaporator. However, the main cycle compressor will still provide the same power. Therefore the main cycle COP increases with additional subcooling.

The subcooling cycle operates between the sink temperature (T_H) and the subcooling cycle evaporator temperature (T_M). Therefore, the COP of the subcooling cycle may be expressed as

$$\text{COP}_{\text{sub}} = \frac{\dot{Q}_{\text{evap,sub}}}{\dot{W}_{\text{sub}}} = \frac{T_M}{T_H - T_M} \quad (3)$$

Neglecting losses to the environment, the subcooling cycle evaporator heat transfer, $\dot{Q}_{\text{evap,sub}}$, is equal to the amount of subcooling provided to the main cycle, \dot{Q}_{sub} .

The overall cycle COP may be expressed as the total refrigeration capacity divided by the total power. The capacity of the overall cycle is simply the capacity of the main cycle without subcooling, plus the increment in capacity of the main cycle due to the subcooling performed. With the assumptions given earlier, the amount of subcooling performed is equal to the increment in capacity to the main cycle, so that $\Delta h_{2-3} = \Delta h_{4-4'}$. The total work performed on the cycle is simply the sum of the compressor work for both the subcooling and main cycles. With these definitions, the COP of the overall cycle may be expressed as

$$\text{COP}_{\text{total}} = \frac{\dot{Q}_{\text{evap,main,no sub}} + \dot{Q}_{\text{sub}}}{\dot{W}_{\text{main}} + \dot{W}_{\text{sub}}} \quad (4)$$

Before this expression may be further manipulated, an assumption is made to model the heat transfer in the subcooler (the only source of irreversibility in the ideal model). The assumption is that the heat transfer in the subcooler is proportional to the temperature difference between the working fluids in the main and subcooling cycles. For the ideal dedicated mechanical subcooling

cycle, the maximum temperature difference in the subcooler is between the sink temperature (T_H) and the subcooling evaporator temperature (T_M). The expression for the subcooler heat transfer can be written as²

$$\dot{Q}_{\text{sub}} = \dot{Q}_{\text{evap,sub}} = \varepsilon C_{\text{min}}(T_H - T_M) \quad (5)$$

where ε is the effectiveness and C_{min} is the minimum capacitance rate, which in this case is the product of the mass flow rate and specific heat of the refrigerant discharged from the main-cycle condenser.

The goal of the ideal model is to develop an expression for the overall cycle COP as a function of the subcooling evaporator temperature, T_M , and system parameters. As T_M is both a measure of the amount of subcooling provided and the subcooling cycle thermal lift, there exists a thermodynamic compromise between the competing effects of increased refrigeration capacity and increased compressor power. The desired expression is obtained by solving Equation (2) for the main-cycle compressor work (which is independent of the amount of subcooling as described earlier), Equation (3) for the subcooling cycle compressor work, and incorporating the subcooler heat transfer (Equation (5)) into Equation (4). The overall COP is then

$$\text{COP}_{\text{total}} = \frac{1 + X \times (T_H - T_M)}{\frac{T_H - T_L}{T_L} + X \times \frac{(T_H - T_M)^2}{T_M}} \quad (6)$$

where X is a measure of the relative size and performance of the subcooler with dimensions of inverse temperature, and may be expressed as

$$X = \frac{\varepsilon C_{\text{min}}}{\dot{Q}_{\text{evap,main,no sub}}} \quad (7)$$

When $T_M = T_H$, Equation (6) reduces to Equation (1), which is the Carnot COP of a cycle operating between T_H and T_L , as expected. If the subcooling evaporator temperature is the sink temperature, there is no temperature difference between the flow streams in the subcooler. Therefore there will be no subcooling provided to the main cycle and consequently no work performed by the subcooling cycle compressor. The overall cycle will then act like one cycle operating between T_H and T_L at the Carnot COP and there will be no advantage to subcooling.

At the lower extreme, $T_M = T_L$, and Equation (6) again reduces to Equation (1). With the subcooling temperature at the refrigerated space temperature, the maximum amount of subcooling is being performed. However, both cycles are now operating over the same thermal lift and the advantage of using dedicated mechanical subcooling is destroyed.

The overall cycle COP in Equation (6) for the ideal model is plotted as a function of the subcooling evaporation temperature T_M and X (Equation (7)) in Figure 3 for $T_L = 230$ K and $T_H = 310$ K. Figure 3 shows that there exists a temperature which optimizes the overall COP, and that this optimum temperature is not strongly affected by the subcooling heat exchanger parameter, X , for the range of values considered. The only major factors influencing the choice of the optimum temperature for the ideal cycle are the sink temperature T_H and the refrigerated space temperature T_L .

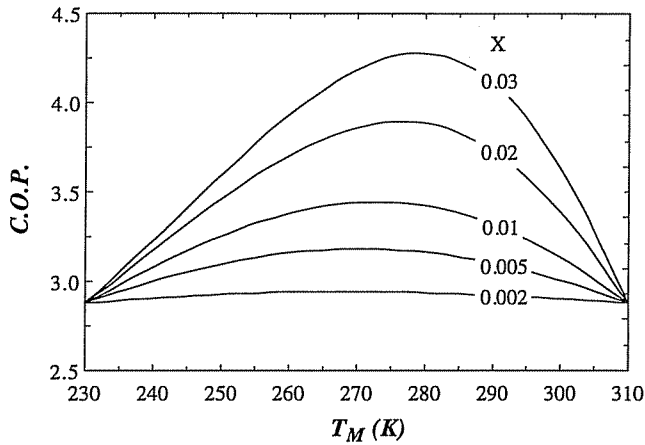


Figure 3 COP as a function of T_M and X for the ideal dedicated subcooling cycle

Figure 3 COP en fonction de T_M et X pour le cycle idéal spécialisé le sous-refroidissement

Optimum temperature for a property-dependent cycle

Although the results for the ideal cycle suggest that an optimum subcooling cycle evaporator temperature exists and that this optimum temperature is dependent only on the sink and refrigerated space temperatures, there are many irreversibilities that could affect the choice of, or even the existence of, the optimum temperature. To evaluate whether the trends developed in the ideal analysis hold for the non-ideal case, a property-dependent computer model of a dedicated subcooling cycle was developed³. A computer simulation was developed for a supermarket application designed to provide 53 kW of low-temperature refrigeration. The property-dependent model accounts for refrigerant thermodynamic properties and the irreversibilities due to compression, expansion and heat exchange. The model was developed using EES, an engineering equation solver that includes built-in thermophysical properties, optimization algorithms and parametric studies⁴. R12 was selected as the refrigerant for this study. The refrigeration system computer model was created by the integration of the steady-state component models discussed below.

Compressors

The steady-state compressor models were based on the concept of an isentropic efficiency as described in ref 5. A reciprocating compressor was assumed with negligible heat transfer to the surroundings. Assuming the compressor to operate reversibly, the ideal (minimum) compressor power for the main cycle is

$$\dot{W}_{\text{comp,main}}^{\text{ideal}} = \dot{m}_{\text{ref,main}}(h_1^{\text{ideal}} - h_5) \quad (8)$$

and

$$s_1^{\text{ideal}} = s_5 \quad (9)$$

Knowing the specific entropy and pressure at ideal state 1 determines the enthalpy, h_1^{ideal} , and thus $\dot{W}_{\text{comp,main}}^{\text{ideal}}$. The actual compressor power is then found using a specified value of the isentropic efficiency, η . The subcooling cycle compressor was modelled in the same

manner. η was assumed to be 0.8 for both the main and subcooling cycle compressors:

$$\dot{W}_{\text{comp,main}} = \frac{\dot{W}_{\text{comp,main}}^{\text{ideal}}}{\eta} \quad (10)$$

Evaporator

In most supermarket applications, the refrigerated display cases act as the evaporators for the refrigeration system. Therefore the refrigerated space temperature dictates the evaporation temperature. Evaporator temperatures of -30°C , -18°C and 7°C were investigated. The refrigerant exiting the evaporator was assumed to leave with 3.9°C of superheat. The evaporator cooling capacity was fixed at 53 kW. The energy balance on the evaporator in Equation (11) fixes the refrigerant flow rate in the main cycle:

$$\dot{Q}_{\text{evap}} = \dot{m}_{\text{ref,main}}(h_5 - h_4) \quad (11)$$

Condensers

The condensers for the main and subcooling cycles were assumed to be air-cooled cross-flow heat exchangers with an air flow rate of approximately $0.12 \text{ m}^3 \text{ s}^{-1}$ per kW of refrigeration, representative of current practice⁶. The condensers were modelled with a fixed UA using a log mean temperature difference (LMTD) based on the condensation temperature, as indicated in Equations (12) and (13) for the main cycle and (14) and (15) for the subcooling cycle, respectively:

$$\begin{aligned} \dot{Q}_{\text{cond,main}} &= \dot{m}_{\text{ref,main}}(h_1 - h_2) \\ &= (UA)_{\text{cond,main}} \text{LMTD}_{\text{cond,main}} \end{aligned} \quad (12)$$

$$\text{LMTD}_{\text{cond,main}} = \frac{(T_{11} - T_{10})}{\ln\left(\frac{T_2 - T_{10}}{T_2 - T_{11}}\right)} \quad (13)$$

$$\begin{aligned} \dot{Q}_{\text{cond,sub}} &= \dot{m}_{\text{ref,sub}}(h_8 - h_9) \\ &= (UA)_{\text{cond,sub}} \text{LMTD}_{\text{cond,sub}} \end{aligned} \quad (14)$$

$$\text{LMTD}_{\text{cond,sub}} = \frac{(T_{12} - T_{10})}{\ln\left(\frac{T_9 - T_{10}}{T_9 - T_{12}}\right)} \quad (15)$$

Expansion valves

A thermostatic expansion valve with negligible heat transfer to the surroundings was assumed for the main and subcooling systems. Thermostatic expansion valves control the refrigerant flow rate in response to the degrees of superheat exiting the evaporator in order to avoid unevaporated refrigerant being passed to the compressor. The valves were considered to be isenthalpic, so that $h_3 = h_4$ and $h_9 = h_6$.

Subcooler

The subcooler was assumed to be a concentric-tube, counterflow heat exchanger. The subcooling heat exchanger acts as the evaporator for the subcooling cycle

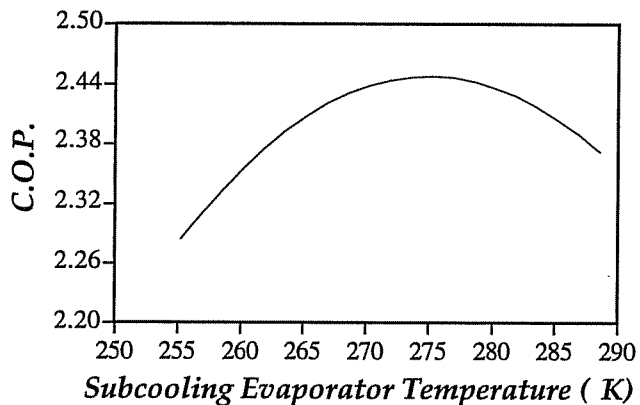


Figure 4 COP as a function of the subcooling evaporator temperature for the property-dependent cycle

Figure 4 *COP en fonction de la température de l'évaporateur de sous-refroidissement pour le cycle idéal*

and the subcooler for the main cycle and was modelled using the LMTD approach with a fixed UA :

$$\begin{aligned} \dot{Q}_{\text{sub}} &= \dot{m}_{\text{ref,sub}}(h_7 - h_6) \\ &= \dot{m}_{\text{ref,main}}(h_2 - h_3) \\ &= (UA)_{\text{sub}} \text{LMTD}_{\text{sub}} \end{aligned} \quad (16)$$

$$\text{LMTD}_{\text{sub}} = \frac{(T_2 - T_3)}{\ln\left(\frac{T_2 - T_6}{T_3 - T_6}\right)} \quad (17)$$

The effect of the subcooling evaporator temperature on overall COP was explored using the property-dependent computer model. The results in Figure 4 show that there is a noticeable maximum point in the COP versus subcooling evaporator temperature plot for a base case, as predicted by the ideal model in Figure 3. However, nine variables could significantly affect the performance of the dedicated subcooling cycle and the choice of the optimal subcooling evaporator temperature. These are:

1. refrigeration load;
2. ambient temperature;
3. degrees of subcooling at exit of evaporators;
4. main cycle evaporator temperature;
5. compressor isentropic efficiency;
6. main cycle condenser UA ;
7. condenser cooling air flow rates;
8. subcooler UA ;
9. subcooling cycle condenser UA .

Of these nine variables, four are constrained by the application to supermarkets and by refrigeration equipment: the refrigeration load, the degrees of subcooling at the evaporator exit, the compressor isentropic efficiency, and the condenser cooling air flow rates. The remaining five variables fall into two groups: heat exchanger size considerations and refrigeration cycle temperature considerations.

Heat exchanger size considerations. The sensitivity of the optimal subcooling evaporator temperature to three heat exchanger sizes (main cycle condenser, subcooling cycle condenser, and subcooler) was explored with the property-dependent computer model. Changing the UA

of any of the heat exchangers ultimately affects the performance of the entire system. The evaporator UA was not considered because it is constrained by the temperature level of the refrigerated case and the specified capacity of 53 kW.

The consequence of changing the UA of all three heat exchangers by the same relative amount was investigated. In this case, the UA product of all three heat exchangers was multiplied by the same constant so that the ratio of each heat exchanger UA to the total remained constant. For this study, the heat exchanger UA products were increased and decreased by 33%. The COP curves in Figure 5 are seen to increase with increasing heat exchanger UA , as expected. However, the sizes of the heat exchangers are seen not to affect the temperature at which the COP is maximum.

The next aspect investigated was whether the relative sizes of the heat exchangers affect the optimal subcooling evaporator temperature. In the base case, the main-cycle condenser UA was 300% greater than the subcooling cycle condenser UA . Figure 6 was generated by decreasing the main cycle condenser UA by 300% and increasing

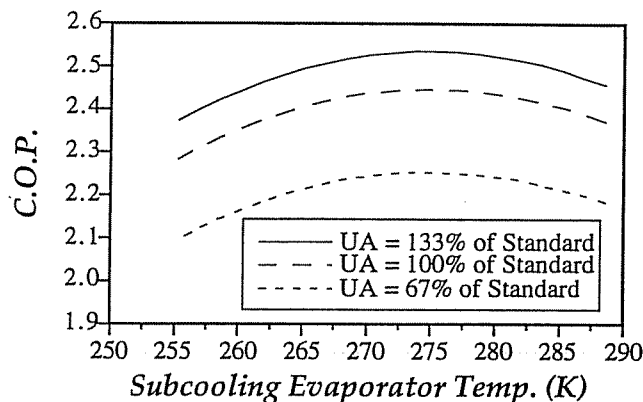


Figure 5 COP as a function of the subcooling evaporator temperature and the total UA product for the property-dependent dedicated subcooling cycle

Figure 5 *COP en fonction de la température de l'évaporateur de sous-refroidissement et du produit KS total pour le cycle auxiliaire de sous-refroidissement (cycle idéal)*

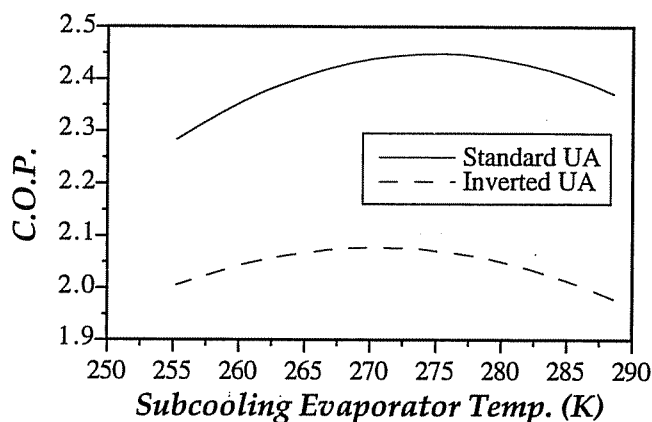


Figure 6 COP as a function of the subcooling evaporator temperature and the condenser UAs for the property-dependent dedicated subcooling cycle

Figure 6 *COP en fonction de la température de l'évaporateur de sous-refroidissement et du KS du condenseur pour le cycle auxiliaire de sous-refroidissement (cycle idéal)*

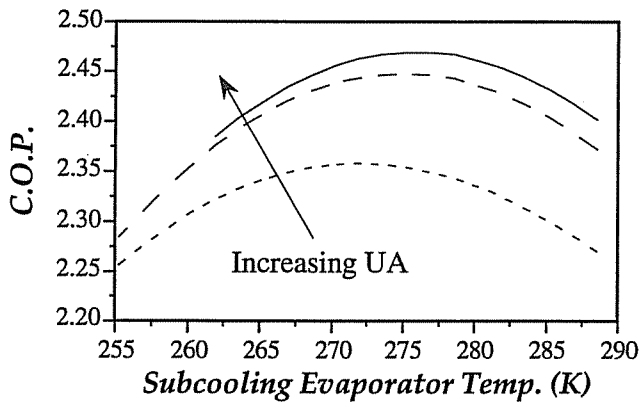


Figure 7 COP as a function of the subcooling evaporator temperature and the subcooler UA product for the property-dependent dedicated subcooling cycle

Figure 7 COP en fonction de la température de l'évaporateur de sous-refroidissement et du produit KS du sous-refroidisseur pour le cycle auxiliaire de sous-refroidissement idéal

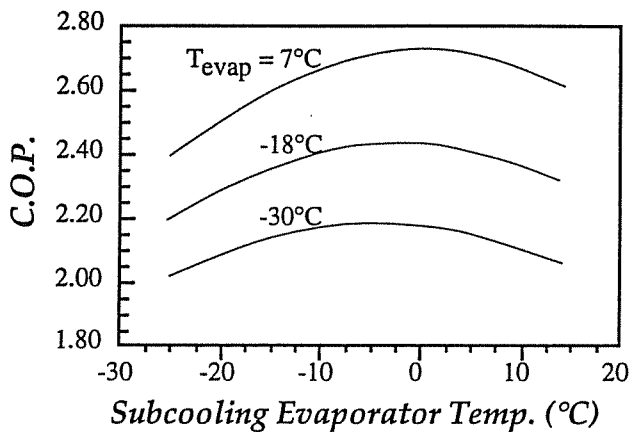


Figure 8 COP as a function of the subcooling and main cycle evaporator temperatures for the property-dependent subcooling cycle

Figure 8 COP en fonction des températures de l'évaporateur du cycle principal et du cycle de sous-refroidissement pour le cycle de sous-refroidissement idéal

the subcooling cycle UA by 300%. The inverted UA labelled on the graph represents the switch from the standard condenser UAs. With the main cycle condenser now being only one-third the size of the subcooling cycle condenser, the COP curves were shifted down by approximately 20%. However, the subcooling evaporator temperature at the maximum COP point was left virtually unchanged. This implies that the maximum COP point is not a strong function of the relative sizes of the condensers.

The ideal model showed that the subcooler heat exchanger size had little effect on the optimal choice of the subcooler evaporator temperature over a range of reasonable values. In the property-dependent case, the UA of the subcooler is seen in Figure 7 to have a slight effect also on the choice of the optimal temperature. The temperature yielding the maximum COP increases with increasing subcooler UA although the variation is small over a wide range of subcooler thermal sizes.

Refrigeration cycle temperature considerations in the

ideal model. The optimum subcooling evaporator temperature was found to increase with increasing main-cycle evaporator and ambient temperatures. Figure 8 shows that the optimum subcooling temperature increases slightly as the evaporator temperature is increased over the normal range of operating temperatures. Figure 9 shows little sensitivity of the optimum subcooling temperature to ambient temperatures.

Model conclusions. The ideal dedicated subcooling model (Equation (6)) exhibits the same tendencies as a property-dependent computer model. The ideal cycle predicts the existence of an optimum subcooling temperature, the importance of the cycle extremes, and the relative unimportance of the heat exchanger's thermal performance on the optimum subcooling evaporator temperature. The ideal model in fact compares well with the property-dependent computer model, regardless of the cycle temperature extremes, as shown in Figures 10 and 11. Even at the upper extreme of main-cycle evaporator temperature, the difference between ideal and property-

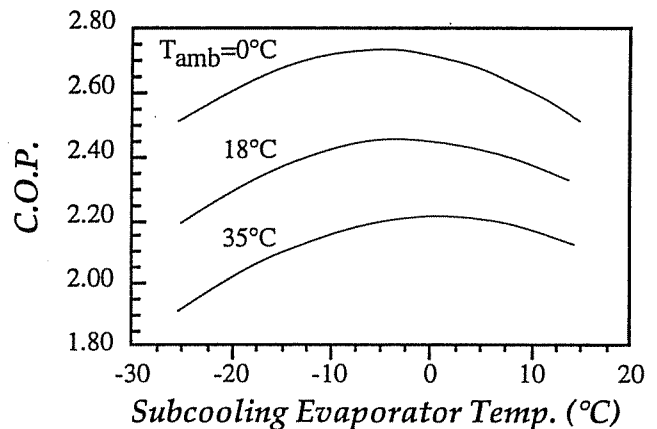


Figure 9 COP as a function of the subcooling evaporator temperature and the ambient temperature for the property-dependent dedicated subcooling cycle

Figure 9 COP en fonction de la température de l'évaporateur de sous-refroidissement et de la température ambiante pour le cycle auxiliaire de sous-refroidissement idéal

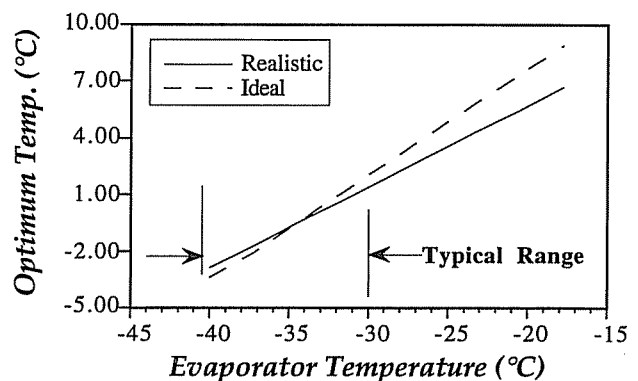


Figure 10 Optimum temperature comparisons between the ideal and property-dependent subcooling cycles as a function of the main cycle evaporator temperature

Figure 10 Comparaisons des températures optimales entre le cycle idéal et le cycle de sous-refroidissement idéal, en fonction de la température de l'évaporateur du cycle principal

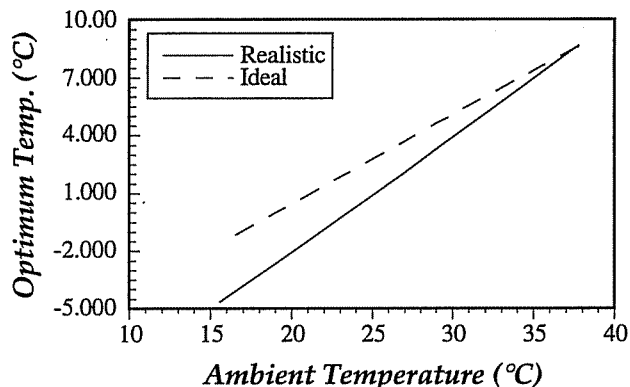


Figure 11 Optimum temperature comparisons between the ideal and property-dependent subcooling cycles as a function of the ambient temperature

Figure 11 Comparaisons des températures optimales entre le cycle idéal et le cycle de sous-refroidissement idéal, en fonction de la température ambiante

dependent estimates was approximately 2.5 °C, corresponding to a change in COP of less than 0.1%.

Design strategies for dedicated subcooling systems

Design considerations for the dedicated subcooling cycle were derived using the property-dependent model. The design considerations were based on an ambient temperature of 26.7 °C, a main-cycle evaporator temperature of -29 °C, and a subcooling evaporator temperature of -1 °C. A subcooling evaporator temperature of -1 °C represents a near-optimal choice for all ranges of ambient and evaporator temperature (Figures 4-9) owing to the relative flatness of the COP curves as a function of the subcooling evaporator temperature near the optimal point. This value is close to the freezing point of water, indicating that ice-storage systems may be good candidates for use in supermarkets to provide subcooling and to offset electrical demand.

For the earlier sections, the UA products of the three heat exchangers (main-cycle condenser, subcooling cycle condenser, and subcooler) were set to values typical of standard practice: a small subcooler, and a subcooling cycle condenser that is a fraction of the size of the main-cycle condenser. However, the question arises as to whether this is the optimal distribution of heat exchange area. This section investigates the optimum UA distribution, develops design guidelines, and evaluates these design guidelines over the range of operating conditions.

As an increase in the total allocated UA product will lead to an increase in the overall cycle COP, the total UA product was constrained to allow the relative effects of heat exchanger distribution to be seen. No attempt was made to determine the optimum total UA as the total allocated UA product should be determined by application and economics. With three unknowns (the three heat exchanger thermal sizes) and one constraint (the total allocated UA product), the problem is reduced to a two-variable optimization.

At the optimum heat exchanger distribution, the subcooler represented approximately 10% of the total allocated UA , which corresponded to a subcooler effectiveness of about 0.95. Also, at the optimum distribution, the main cycle condenser UA was 3.3 times as large as the subcooling cycle condenser UA , with

effectiveness values of 0.665 and 0.717 respectively. Therefore the subcooler is seen to be the critical heat exchanger in the dedicated subcooling cycle. The optimization was done using the algorithms in the EES program.

The results, however, are based on assumed conditions of a 26.7 °C ambient temperature and a -29 °C evaporator temperature, which are the only major factors influencing the choice of the optimum subcooling evaporator temperature. These temperatures are also the only major factors influencing the optimum heat exchange distribution. As seen in Figures 12 and 13, the optimum subcooler UA is unaffected by ambient and evaporator temperatures. The optimum UA for the condenser in the subcooler cycle increases with increasing ambient temperature but is unaffected by the evaporator temperature. The heat exchanger distribution results can be summarized as follows.

1. The optimum subcooler UA is unaffected by the choice of ambient temperature and only slightly affected by the choice of evaporator temperature.
2. The ratio of main-cycle condenser size to subcooling cycle condenser size decreases as the ambient temperature increases.

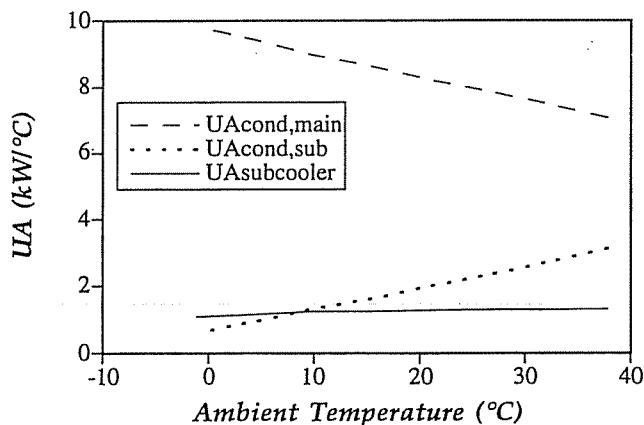


Figure 12 Optimum heat exchanger distribution as a function of the ambient temperature

Figure 12 Répartition optimale des capacités des échangeurs thermiques en fonction de la température ambiante

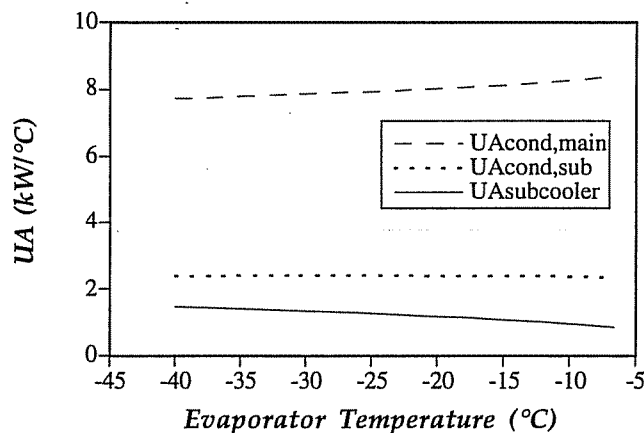


Figure 13 Optimum heat exchanger distribution as a function of the main-cycle evaporator temperature

Figure 13 Répartition optimale des capacités des échangeurs thermiques en fonction de la température de l'évaporateur de cycle principal

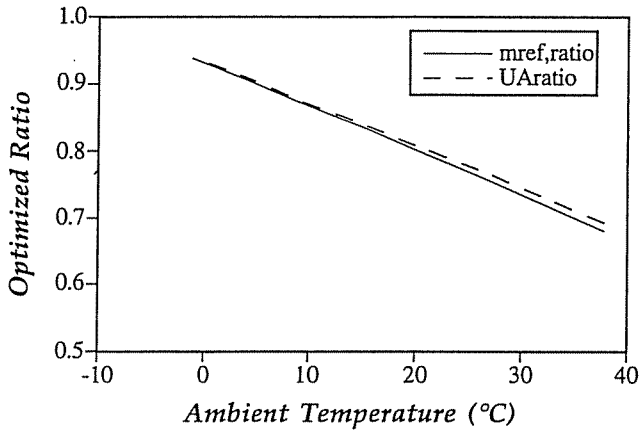


Figure 14 Optimized ratios as a function of the ambient temperature
 Figure 14 *Rapports optimisés en fonction de la température ambiante.*

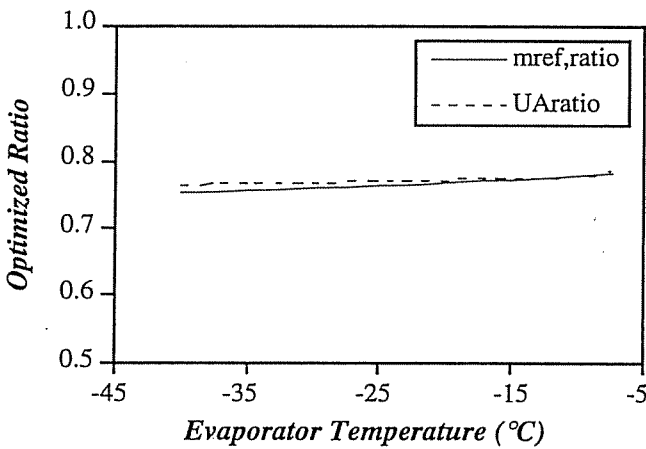


Figure 15 Optimized ratios as a function of the main cycle temperature
 Figure 15 *Rapports optimisés en fonction de la température du cycle principal*

3. The ratio of main-cycle condenser size to subcooling cycle condenser size decreases as the evaporator temperature decreases.

The refrigerant flow rate ratio was determined and compared with the *UA* ratios at the optimum. These ratios are defined as

$$\dot{m}_{\text{ratio}} = \frac{\dot{m}_{\text{ref,main}}}{\dot{m}_{\text{ref,main}} + \dot{m}_{\text{ref,sub}}} \quad (18)$$

and

$$UA_{\text{ratio}} = \frac{UA_{\text{cond,main}}}{UA_{\text{cond,main}} + UA_{\text{cond,sub}}} \quad (19)$$

An important trend is revealed when the refrigerant flow rate ratio and the optimized *UA* ratio are plotted as functions of the ambient and evaporator temperatures. Figures 14 and 15 show that the optimum *UA* ratio (which is a direct measure of the optimum heat exchange distribution) closely matches the refrigerant flow rate regardless of ambient or evaporator temperature.

Design guidelines for a dedicated mechanical subcooling system can be established using trends developed from the property-dependent computer model.

1. Select the total *UA* product available for the dedicated subcooling system based on economics.
2. Apportion approximately 10% of the allocated heat exchange area to the subcooler, which corresponds to a high value of the subcooler heat exchanger effectiveness, eg 0.95.
3. Distribute the remaining *UA* product according to the expected refrigerant flow rates at this 'design' temperature.

Conclusions

An ideal mechanical subcooling cycle was developed from Carnot theory and heat transfer relations. This ideal cycle predicted the existence and location of the 'optimum' subcooling temperature for the dedicated subcooling cycle. The ideal cycle also predicted that the 'optimum' temperature was strongly dependent on the sink and refrigerated space temperatures, and weakly dependent on the subcooler heat exchanger parameters. A model of a property-dependent dedicated subcooling cycle was developed. The property-dependent model accounted for the irreversibilities due to compression, expansion and heat exchange. The property-dependent model showed the same trends predicted by the ideal model: the existence and location of an 'optimum' subcooling evaporator temperature, the strong dependence on cycle temperature extremes, the weak dependence on subcooler heat exchanger parameters, and the relative unimportance of the condenser thermal sizes.

The property-dependent model allowed the optimal heat exchanger distribution to be developed, and design guidelines to be established. The improvement in overall COP through the use of a subcooler was found to be approximately 10% over a range of conditions representative of supermarket applications. The optimum heat exchanger distribution and design guideline for a dedicated subcooling cycle can be summarized as follows.

1. As the subcooler thermal size is relatively independent of ambient and main-cycle evaporator temperatures, apportion 10% of the allocated *UA* product to the subcooler.
2. Although the ratio of main-cycle condenser thermal size to subcooling cycle thermal size decreases as the cycle temperature extremes increase, the ratio of the condenser *UAs* mirrors the ratio of refrigerant flow rates. Therefore the optimal distribution of condenser thermal sizes will be in the same ratio as the design refrigerant flow rates.

References

- 1 Couvillion, R. J., Larson, M. W., Somerville, M. H. Analysis of a vapor-compression refrigeration system with mechanical subcooling *ASHRAE Trans* (1988) 94(2) 641-659
- 2 Incropera, F. P., DeWitt, D. P. *Introduction to Heat Transfer* John Wiley and Sons, New York (1985)
- 3 Thornton, J. Supermarket refrigeration options *MS Thesis* Dept of Mechanical Engineering, University of Wisconsin-Madison (1991)
- 4 Klein, S. A., Alvarado, F. L. *EES: Engineering Equation Solver* F-Chart Software, Middleton, WI (1991-1994)
- 5 Van Wylen, G. J., Sonntag, R. E. *Fundamentals of Classical Thermodynamics* John Wiley and Sons, New York (1986)
- 6 *ASHRAE Handbook, Equipment Volume* American Society of Heating, Refrigeration, and Air-Conditioning Engineers Inc., Atlanta, GA (1983)

A new method to determine the heat transfer coefficient of refrigerated vehicles

Guimei Zhang* and Guichu Sun

Department of Transportation, Northern Jiaotong University, Beijing 100044, PR China

Jiankun Li

Sifang Rolling Stock Institute, 12 Jiaxin Road, Qingdao 266031, PR China

Received 19 November 1992; revised 7 February 1994

A new method is proposed for rapid determination of the overall heat transfer coefficient K of refrigerated and insulated vehicles. By calculating the temperature distribution in the insulation wall using the finite difference method, the following parameters were obtained: the heat inertness coefficient and the conversion ratio. A new formula for calculating the K -value is based on these parameters. The principle and experiments are discussed and analysed in detail in this paper. The results show that the time required by the new method is less than that required by other rapid methods, while the precision is much higher. Compared with the steady-state method, the error is within a limit of 5%. This new method is particularly suited to quality control testing of vehicles in production runs.

(Keywords: refrigerated transport; wall; insulation; K coefficient; simulation; calculation)

Nouvelle méthode pour déterminer le coefficient de transfert de chaleur des véhicules frigorifiques

On propose une nouvelle méthode pour déterminer rapidement le coefficient de transfert de chaleur global K des véhicules réfrigérés et isothermes. En calculant la distribution de température dans le mur isolant, en utilisant la méthode des différences finies, on a obtenu les paramètres suivants: un coefficient d'inertie à la chaleur et un taux de conversion. Une nouvelle formule pour calculer la valeur K se fonde sur ces paramètres. On examine en détail le principe et les expériences effectuées. Les résultats montrent que cette nouvelle méthode est d'une utilisation plus longue que les autres, mais qu'elle est plus précise. Par rapport à la méthode en régime stable, le pourcentage d'erreur est de 5%. Cette nouvelle méthode convient particulièrement bien pour les essais sur le contrôle de la qualité des véhicules, dans les usines de production.

(Mots clés: transport frigorifique; paroi; isolation; coefficient K ; simulation; calcul)

The production supervision of refrigerated and insulated vehicles is performed in various ways. On body production lines, a sample of about 1% of 'prototypes' is tested in the laboratory; 3 days are needed for this process. About 1% of samples are also tested in the workshop, using a rapid method.

Several rapid methods are available for determining the K -value¹⁻¹¹; however, the precision of these methods is unsatisfactory, because they neglect the unsteady temperature distribution in the insulating material. By calculating the temperature distribution, we have obtained some parameters that may be used to set up a new formula for obtaining improved test results in less time.

Principles

Unsteady-state methods

Unsteady-state methods are based on the equation $Q = KA\theta + W d\theta/d\tau$, from which various formulae for calculating the K -value have been derived.

*Putz's method*¹. Putz, using the instantaneous heat transfer coefficient $K_s = Q/A\theta$, hypothesizes $K_s = a + be^{-\tau} + ce^{-0.1\tau}$; when $\tau \rightarrow \infty$, $K_s = a$. Using Gauss' least-square method, he obtains

$$a = \frac{A(BE - CC) - G(DE - CF) + H(CD - BF)}{n(BE - CC) - D(DE - CF) + F(CD - BF)}$$

where $A = [K_i]$, $B = [e^{-2\tau}]$, $C = [e^{-1.1\tau}]$, $D = [e^{-\tau}]$, $E = [e^{-0.2\tau}]$, $F = [e^{-0.1\tau}]$, $G = [K_i e^{-\tau}]$, $H = [K_i e^{-0.1\tau}]$, and n is the number of measured points. $[e^{-\tau}]$ is the sum of all $e^{-\tau}$; the rest of the bracketed terms may be derived analogously.

*Kriha's method*². Kriha determines $d\theta/d\tau$ of two points in the temperature-time curve and obtains

$$K = K_{s1} - \frac{W}{A\theta_1} \left(\frac{d\theta}{d\tau} \right)_1$$

$$W = \frac{A(K_{s1} - K_{s2})}{\frac{1}{\theta_1} \left(\frac{d\theta}{d\tau} \right)_1 - \frac{1}{\theta_2} \left(\frac{d\theta}{d\tau} \right)_2}$$

*Present address: Federal Research Centre for Nutrition, Institute of Process Engineering, Engesserstr. 20, 76131 Karlsruhe, Germany